STEM CELLS AND DEVELOPMENT 16:1–14 (2007)

DOI: 10.1089/scd.2007.0026

MicroRNA Expression Pattern of Undifferentiated and Differentiated Human Embryonic Stem Cells

UMA LAKSHMIPATHY,[1] BRAD LOVE,[1] LOYAL A. GOFF,[2] REBECKA JÖRNSTEN,[3] RALPH GRAICHEN,[4] RONALD P. HART,[2] and JONATHAN D. CHESNUT[1]

ABSTRACT

Many of the currently established human embryonic stem (hES) cell lines have been characterized extensively in terms of their gene expression profiles and genetic stability in culture. Recent studies have indicated that microRNAs (miRNAs), a class of noncoding small RNAs that participate in the regulation of gene expression, may play a key role in stem cell self-renewal and differentiation. Using both microarrays and quantitative PCR, we report here the differences in miRNA expression between undifferentiated hES cells and their corresponding differentiated cells that underwent differentiation in vitro over a period of 2 weeks. Our results confirm the identity of a signature miRNA profile in pluripotent cells, comprising a small subset of differentially expressed miRNAs in hES cells. Examining both mRNA and miRNA profiles under multiple conditions using cross-correlation, we find clusters of miRNAs grouped with specific, biologically interpretable mRNAs. We identify patterns of expression in the progression from hES cells to differentiated cells that suggest a role for selected miRNAs in maintenance of the undifferentiated, pluripotent state. Profiling of the hES cell "miRNA-ome" provides an insight into molecules that control cellular differentiation and maintenance of the pluripotent state, findings that have broad implications in development, homeostasis, and human disease states.

INTRODUCTION

EMBRYONIC STEM (ES) CELLS share several unique features, including unlimited self-renewal and the ability to differentiate into any of the three embryonal lineages—ectoderm, endoderm, and mesoderm. For the cell fate decision to be made in response to internal and/or niche-specific signals, a complex set of dynamic feedback loops and cross-regulation of pathways is required (1,2). In addition to feedback loops, regulation by methylation of CPG islands has been proposed (3,4). This is critical in X chromosome inactivation and imprinting of specific gene loci, and it may be important in regulating expression of ES cell-specific genes (5,6). Additional microRNA (miRNA)-directed regulatory pathways have been proposed including those regulating the timing of differentiation. None of these pathways has been explored rigorously, although a recent convergence of technologies allowing isolation of sufficient amounts of purified cells for analysis and various large-scale analytical methods have made these types of studies more feasible.

For instance, hES cells can now be maintained in feeder-independent cultures in an undifferentiated state and be used to obtain robust differentiation via the addition of exogenous reagents to the culture media (7,8). Although cell culture techniques and media additives have contributed much to our knowledge of stem cell differentiation and maintenance of pluripotency, significant

[1]Invitrogen Corporation, Carlsbad, CA 92008.
[2]W.M. Keck Center for Collaborative Neuroscience, and [3]Department of Statistics, Rutgers University, Piscataway, NJ 08854.
[4]ES Cell International Pte, Ltd., Singapore 138667.

work needs to be done to understand the molecular mechanisms involved in these processes. Global mRNA expression and methylation profiling of various hES cell lines have been well characterized (3,9–14). More recently, miRNA expression in stem cells has been shown to differ significantly from other cell types tested to date (15–17).

miRNAs are short (20- to 24-nucleotide), noncoding RNAs that have been identified in various organisms including mammalian cells. The sequence of most miRNAs are highly conserved across species, with nearly 90% of the currently sequenced human miRNAs identical to mouse and rat and at least 30% homologous to miRNAs from *Caenorhabditis elegans* (18). miRNAs are thought to regulate gene expression negatively by direct mRNA cleavage (19–23), mRNA decay by deadenylation (24,25), or translational repression (26). To complicate the specific mapping of miRNA binding sites in the transcriptome, it has been determined that, at least in animal cells, translational repression occurs by annealing of miRNA to mRNA at sites with imperfect complementarity (27). Due to this complexity and the lack of a clear understanding of the mode of action of miRNA function, the identification of target mRNAs regulated by miRNA has been difficult (28). Nevertheless, the importance of miRNA in several biological processes such as cell growth and apoptosis (29), viral infection (30), and human cancer (31–33) is well documented. On the basis of several studies, it has been suggested that miRNAs regulate gene expression of more than 30% of protein-coding genes in humans (34). The role of miRNA-mediated regulation of stem cell division (35), as well as adipocyte (36), cardiac (37), neural (28,38) and hematopoietic lineage differentiation (21,39) is well known. More recently, a unique set of miRNAs has been shown to be associated with mouse ES cells and embryoid body (EB) formation (15,17,40–42). Using northern blot analysis and cloning, several miRNAs were identified in hES cells, of which several were identical to miRNAs previously reported in mouse ESCs (16). Consistent with this observation, a mouse ES cell knockout lacking Dicer (40) and DGC8 (43), two key processing enzymes in miRNA biosynthesis, exhibit a failure to undergo differentiation, further implicating their importance as key regulators during this process.

Methods for gene expression analysis have been available for some time and are now widely used in the field. Recently, tools for systematic analysis of epigenetic changes in cells have become available, opening the door for broad-scale analysis on another level of transcriptional and translational regulation. In this study, NCode™ miRNA arrays (44) and quantitative PCR were used to analyze miRNA profiles of various hES cell lines and their differentiated cells derivatives. We show here that although there are some informative variations in the miRNA profiles between hES cell lines, there are also several markers that are highly expressed across all hES cell lines tested in this study. Furthermore, as these cells differentiate, the miRNA profiles change significantly. Using a semiquantitative assay, miRNA copy numbers were estimated across pluripotent hES cells, differentiating cells, and adult human brain, a representative sample of terminally differentiated adult tissue. Finally, gene expression and miRNA expression were correlated to identify potential regulators of key pluripotent genes. The results of this study will form the basis for further perturbation studies to study epigenetic regulation of miRNA to determine stem cell fate.

MATERIALS AND METHODS

ES cell culture

hES cells lines CyT25 and CyT203, cultured and differentiated as previously described (45), were kindly provided by Melissa Carpenter, Novocell. hES cells lines (HES2, HES3, and HES4) were from ES Cell International (http://stemcells.nih.gov/research/registry/esci.asp) at passage numbers ranging between 75 and 125 and with a normal karyotype; they were cultured and differentiated as described previously (46,47). In short, hES cells were cultured on a mitotically inactive in-house-derived mouse embryonic fibroblast (MEF) feeder layer using gelatin-(Sigma) coated culture dishes (Falcon). Culture medium was changed daily and was composed of Dulbecco's modified Eagle medium (DMEM; with or without glucose and sodium pyruvate respectively; Invitrogen), supplemented with 20% fetal bovine serum (FBS), 0.1 mM β-mercaptoethanol (Invitrogen), 1% nonessential amino acids (Invitrogen), 2 mM L-glutamine (Invitrogen), 1% insulin-transferrin-selenium (Invitrogen), and 50 IU/ml penicillin and 50 μg/ml streptomycin (Invitrogen). Cells were subcultured every 7 days by mechanical microdissection. For differentiation, cells were washed once with phosphate-buffered saline (PBS) and treated with collagenase IV (1 mg/ml) for 3–4 min at 37°C. Collagenase was replaced by serum-free (SF) medium [DMEM medium supplemented with 1% minimum essential medium (MEM) nonessential amino acids, 2 mM L-glutamine, 1× ITS, 0.1 mM β-mercaptoethanol, and penicillin/streptomycin], and culture plates were scored with a 10-μl pipette tip (Eppendorf). The entire adherent cell layer was scraped off using a cell scraper (Iwaki) and the cell suspension transferred to a 50-ml tube (Falcon) and allowed to settle. The cell pellet was then resuspended in fresh SF medium and briefly triturated before an equal volume of cell suspension was transferred to ultra low attachment six-well plates (Costar). Medium changes of EBs were

performed every 3 days for a period of 12 days prior to harvesting EBs for analysis.

The culture and maintenance of BG01V and hUES cells were as described earlier (48). Briefly, BG01V cells from BresaGen Inc. (San Diego, CA; http://www.novocell.com) were routinely passaged on CF1-inactivated MEFs in DMEM/F12 media containing 15% FBS and 5% Knockout Serum Replacement (Invitrogen), glutamine, nonessential amino acids, β-mercaptoethanol and 4 ng/ml basic fibroblast growth factor (bFGF). Cells were replenished with fresh medium daily, and cells were passaged every 4–5 days using collagenase IV. HUES lines HUES 20 and HUES21, obtained from Harvard University, were cultured as instructed (https://www.mcb.harvard.edu/melton/hues), and cell pellets were provided by Jonathan Auerbach (GlobalStem, USA).

Ntera2 cl D1 cells were obtained from the American Type Culture Collection (ATCC) (ATCC CRL-1973), and 2102Ep was provided by Peter W. Andrews (Sheffield, UK). Cells were grown under high density in tissue culture dishes in growth medium containing DMEM supplemented with 10% FBS. The growth medium was changed daily, and cells were passaged every 3–4 days by gently scraping the cells off the dish.

RNA isolation

Total RNA was isolated using Trizol Reagent (Invitrogen) according to manufacturer's instructions. Contaminating genomic DNA was removed from the isolated RNA by treatment with amplification-grade DNase I (Invitrogen) for 2 h at 37°C. RNA was precipitated and quantified spectrophotometrically, and its purity was assessed by electrophoresis on a 15% Nupage urea-TBE gel (Invitrogen).

Gene expression using microarrays

For Illumina BeadArray, total RNA was amplified and labeled as reported earlier (11). Labeled, amplified material (~700 ng per array) was hybridized to the Illumina HumanRef-8 v2 BeadChip according to the manufacturer's instructions (containing >22,000 probes based on the Human RefSeq database, Illumina, Inc., San Diego, CA). Array data processing and analysis was performed using Illumina BeadStudio software.

Enrichment of miRNA

miRNA was isolated from Trizol-extracted total RNA using Purelink miRNA Isolation Kit (Invitrogen) according to recommended protocol. The amount of miRNA was quantified spectrophotometrically, and its purity was assessed by electrophoresis on a 15% Nupage urea-TBE gel (Invitrogen).

Ncode™ miRNA array

To compare global miRNA expression between hES cells and their EB, a heterotypic dye swap experiment was carried out using the NCode™ miRNA array. Five hundred nanograms of the enriched miRNA was labeled with the Ncode™ direct labeling system and hybridized to replicate NCode™ multispecies miRNA arrays (44) as described earlier (48). Briefly, hES cell miRNA fraction was labeled with Alexa 3 dye (green) and the corresponding differentiated cell miRNA fraction was labeled with Alexa 5 (red). A second slide reversed the dyes, with hES cells labeled with Alexa 5 (red) and the differentiated sample with Alexa3 (green). Because the miRNA probes are printed in duplicate on the NCode array, a total of four data points for each miRNA can be obtained with minimal sample and slides. The identified markers were subsequently validated by the more sensitive and quantitative method of miRNA quantitative PCR using the unamplified total RNA from all the five hES cells and their differentiated cells.

NCode™ quantitative PCR

Quantitative PCR was performed on unamplified total RNA using the NCode™ quantitative PCR kit (Invitrogen) as described earlier (49). The differences in miRNA expression between samples were determined using the relative quantification method. Briefly, the C_t values of the samples were normalized to the C_t values of glyceraldehyde 3-phosphate dehydrogenase (GAPDH), a housekeeping gene. The resulting values were further normalized to 2102Ep human embryonic carcinoma cells, which were used as a reference cell line. The fold difference in gene expression of the sample from the reference 2102Ep cells was calculated using the equation $2^{-\Delta\Delta Ct}$. To assign miRNA copy numbers, a standard curve was generated from a pure synthetic template diluted over several logs. The C_t values of the reference 2102Ep cell line were converted to copy number based on fold differences of each miRNA obtained using the relative quantification method. Therefore, the copy number generated is a relative approximation and not absolute numbers.

Correlation of mRNA and miRNA expression

Samples of hES cell cultures were classified a priori into three biological groups—ES cells, differentiated ES cells (EB), or embryonic carcinoma (EC) cells. Illumina data were quantile normalized (50) and filtered for genes with a detection threshold of at least 0.99 under one or more conditions. NCode and Illumina array data were normalized and corrected for experimental effects using

a linear model (51). Briefly, the following linear model was fit to the log-expression profile of each gene:

$$Y_{ijkg} = \mu + A_i + D_j + V_k + G_g + AG_{ig} + VG_{kg} + \varepsilon_{ijkg}$$

where A, D, V, and G represent the additive effect of the i^{th} array, j^{th} dye, k^{th} biological group, and g^{th} gene, respectively; AG represents the combinatorial effect of the i^{th} array with the g^{th} gene, effectively modeling any chip or spot artifacts; ε_{ijkg} describes the random error associated with each measurement; and VG represents the combinatorial effect of the k^{th} biological group with the g^{th} gene. This last effect, VG, is used to interpret any gene expression differences between the biological groups. All additive effects were estimated via least squares. An F-test was performed on the modeled data, with or without VG_{kg} effects, to select differentially expressed genes. The p values were obtained via bootstrapping and adjusted for multiple comparisons using the Benjamini–Hochberg method (52), with a tolerated false discovery rate of 5%. The miRNA/mRNA data were examined jointly by computing pairwise correlations between the estimated VG_{kg} effect profiles. Heat map displays were constructed from these correlation matrices using the heatmap.2 function from the gplots library in the statistical software R (http://www.r-project.org). Target predictions were identified from a downloaded database of RNA22 predictions (53) using ENSEMBL transcript identifiers to link Illumina probes as predicted miRNA targets.

RESULTS

Global mRNA expression profiles of ES cells and EBs

As a first step, we sought to characterize the hES cell lines and their differentiated cells used in the study. Gene expression analysis was carried out using Illumina bead array as described previously (54). Prior to consideration of the data, the quality of each array was confirmed by comparing the signal intensity distribution obtained for each sample. The entire set of gene expression data and a table showing the signal intensity distribution is provided in Supplementary Table 1 (accessible at http://cord.rutgers.edu/appendix/Supplemental_Table_1.xls). Samples were then compared pairwise by creating a scatter plot of expressed genes with a detection level greater than 0.99. Pairwise comparison of two samples with a correlation coefficient (R^2) value closer to 1.0 indicates similarity in transcript expression between the two cell types whereas a variation of transcript expression by over two-fold is reflected by a lower correlation value. For example, the R^2 value between the two hES cell lines CyT25 and CyT203 is 0.938 (Fig. 1A). This value is however decreased 0.839 when the hES cell line CyT203 is compared to its corresponding differentiated cells (Fig. 1B). A similar decrease in the correlation value is observed for all the five hES cells upon differentiation indicating a change in the expression level of a significant number of transcripts between hES cells and their corresponding differentiated cells (not shown). It is interesting to note here that HES2, HES3, and HES4 show a correlation R^2 value close to 1. However, the R^2 value between HES2 and CyT203 is 0.858, indicating that the HES lines are more similar to each other than compared to CyT203. This may be largely due to cell culture conditions because the cell maintenance and differentiation protocols were different for these two sets of samples. Nevertheless, comparison of the ES cells with their corresponding differentiated cells does indicate a change in transcript expression reflected by the decrease in the correlation (R^2) value. On the basis of global gene expression profiles, the relatedness of samples is plotted as a dendrogram (Fig. 1C).

Although there is some variation in the gene expression profiles between different hES cells lines, there are sets of genes that are known to be regulated during the very early stages of differentiation. To confirm uniform differentiation of all the hES cells lines used in this study, the expression levels (expressed as arbitrary signal units) of pluripotency markers [Oct4 (POU5F1), Nanog, Rex1 (ZFP42), UTF1 and TDGF1] and markers for general differentiation [HAND 1, AFP and OTX1; specific for mesoderm, endoderm and ectoderm, respectively] (54) were measured. The expression of Oct-4 decreased after differentiation more prominently (>100-fold) for HES2, HES3, and HES4 compared to CyT25 and CyT203 (2- to 3-fold). Consequently, an increase in the signal for the differentiation markers is apparent in differentiated cells relative to the parent hES cells line (Table 1). The decrease in pluripotency-associated genes together with an increase in general differentiation marker expression indicates differentiation of all the hES cell lines after differentiation.

Global miRNA expression profiles of ES cells and EBs

The expression profiles of 55 human miRNAs determined to be significantly regulated between ES, EB, and EC biological groups are sufficient to separate samples into biologically interpretable groups (Fig. 2). Biological replicates are appropriately grouped to indicate technical proficiency. Interestingly, in contrast to the relationships deduced from mRNA expression profiles, the CyT25 and CyT203 samples are interdispersed among the hES cell samples, suggesting a closer relationship to the ES cells when comparing miRNA profiles across all cell samples, including carcinomas (Ntera and 2102Ep samples). The differences between the differentiated CyT25 samples and the undifferentiated CyT25 samples are less drastic

than those observed between the undifferentiated and differentiated CyT203. Ntera2 and 2102Ep samples, while both classified in this study as EC cells, cluster with distinct subsets of the ES group, suggesting that miRNA profiles classify samples on the basis of an unexpected relatedness between these cell types.

Select miRNAs or groups of miRNAs can readily be identified within the significance list, and their relationships among samples illustrate several interpretations. For example, miR-17 cluster members (33) appear to be enriched in Ntera2 and differentiated EB samples, as well as select ES samples, suggesting they may be further along the differentiation path. miR-302, a previously described ES cell-specific marker (15,16), appears enriched in all samples, although slightly less so in the Ntera2 group. let-7 family members are more highly enriched in all of the HUES samples as well as the BGOV1. miR-21, a miRNA previously associated with tumorigenesis (55,56) is elevated in Ntera2, BG0V1, and HUES20 cell lines. miR-9, a miRNA associated with the neuronal phenotype (57), is elevated in the Ntera2 cell line. In several other cases, tissue-specific/enriched miRNAs are restricted to subsets of ES/EB/EC cell types. Clearly, miRNA expression patterns are informative and allow a novel classification of samples using this set of parameters.

The entire NCode miRNA expression data and signal in-

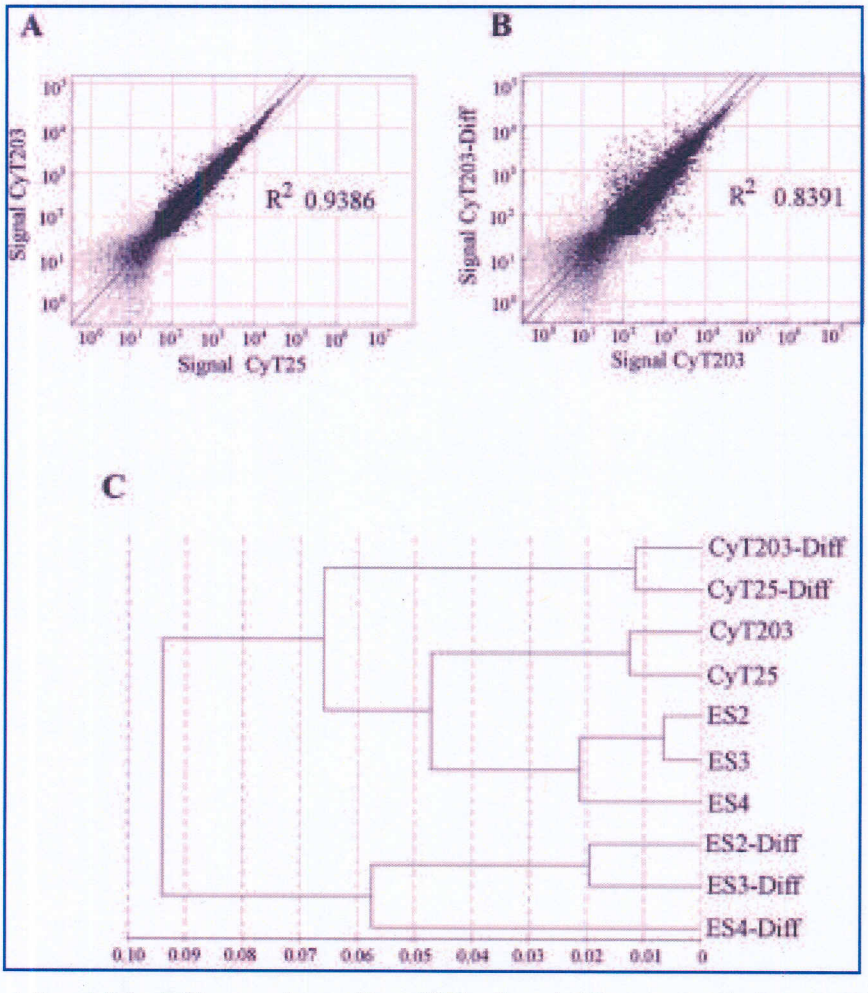

FIG. 1. Representative global mRNA expression profiles of hES cells and differentiated cells. Total RNA isolated from the three hES cells cell lines HES2, HES3, and HES4 and their corresponding cells after 12 days of differentiation were used for mRNA expression analysis using the Illumina bead array. Data were analyzed using Bead Studio software, and data points representing greater than a 0.99 detection threshold are represented as points in the scatter plot. Points lying outside the lines represent genes with greater than two-fold difference and R^2 value closer to 1 suggest similar gene expression pattern. (**A**) Comparison of global gene expression between two hES cells lines CyT25 and CyT203 with a correlation (R^2) value of 0.938. (**B**) Comparison of global gene expression between CyT203 and its CyT203-differentiated cell for 2 weeks with a correlation (R^2) value of 0.839. (**C**) Dendrogram showing relatedness in global gene expression of the hES cells and differentiated samples.

TABLE 1. SIGNAL INTENSITY OF KEY PLURIPOTENT AND DIFFERENTIATION MARKERS IN ES CELLS AND DIFFERENTIATED CELLS SAMPLES OBTAINED ON ILLUMINA GENE ANALYSIS CHIP

		hES cells					*Differentiated cells*				
Specificity	*Genes*	*CyT25*	*CyT203*	*ES2*	*ES3*	*ES3*	*CyT25-Diff*	*CyT203-Diff*	*ES2-Diff*	*ES3-Diff*	*ES3-Diff*
Pluripotent	POU5F1	**701**	**763**	**408**	**486**	**369**	343	480	36	5	8
	NANOG	**89**	**133**	**141**	**158**	**66**	75	107	−12	−13	5
	ZFP42	**2,048**	**2,715**	**1,168**	**1,218**	2	925	950	144	141	**27**
	UTF1	**1,208**	**1,880**	**614**	**402**	**362**	117	134	38	38	31
	TDGF1	8,387	**10,858**	**5,967**	**5,390**	**5,767**	**10,881**	9,530	92	63	64
Differentiation	HAND1	158	217	138	3,017	27	**1,233**	**1,748**	**15,147**	**11,743**	**3,206**
	AFP	297	83	187	292	148	**714**	**684**	**27,189**	**22,294**	**9,497**
	OTX1	−1	11	20	12	2	**17**	**31**	**292**	**143**	**168**

The intensity, represented as arbitrary units, is represented in bold when the value is greater between ESC and their corresponding EB.

tensity distribution is provided as Supplementary Table 2 (accessible at http://cord.rutgers.edu/appendix/Supplemental_Table_2.xls). To quantitatively measure the differences in the miRNA levels between ES and EB samples further, a list of miRNA candidates differentially expressed between ES and EB (with p values less than 0.02) along with markers expressed similarly in ES and EB and earlier reported miRNAs associated with hES cells (16) were chosen for further validation by quantitative PCR of all the five hES cells samples and their corresponding EBs.

miRNAs expression between hES cells and differentiated cells

To determine if a subset of significantly regulated miRNAs are useful to classify hES cells and their differentiated products, we assayed three new hES cells preparations (ES2, ES3, and ES4) by quantitative PCR. Analysis of the chosen group of miRNAs differentially expressed between the three hES cells lines and their corresponding differentiated cells was carried out using total cellular RNA fractions. Because no specific miRNAs have been identified to be expressed at consistent levels across all cell lines (i.e., potential housekeeping miRNAs), miRNA quantitative PCR values in this study were normalized to the GAPDH mRNA transcript. These values were further normalized to miRNA levels in reference to the nullipotent human EC line 2102Ep (48). We chose this cell line to serve as a reference standard for pluripotent cells to allow for normalization between data sets obtained during multiple quantitative PCR runs (Supplementary Table 3, http://cord.rutgers.edu/appendix/Supplemental_Table_3.xls). Data are presented as a heat map of the fold change relative to 2102Ep cells with higher expression levels represented as red and lower expression levels represented as green (Fig. 3). With the three newly tested ES lines (ES2, ES3, and ES4), the selected miRNAs correctly cluster the samples by differentiation status. The CyT25 and CyT203 ES and EB samples were also clustered by cell phenotype. The quantitative PCR miRNA expression patterns correctly distinguished ES from EB states for each cell line.

Whereas relative expression values provide a clear indication of differential expression, the absolute level of expression (copy number) of each miRNA itself is a more useful measure of miRNA concentration dif-

FIG. 2. Representative global miRNA expression heat map of hES cells and differentiated cells (day 12). Significantly regulated miRNAs were examined for expression levels in all samples by drawing a hierarchically clustered heat map with associated dendrograms. Colors represent $\log_2$ expression values as depicted in the color key (*inset*). In general, technical replicates clustered together tightly as expected. The two embryonic carcinoma (EC) lines (Ntera and 2102Ep) cluster with distinct ES cell lines, suggesting that miRNAs identify a range of cell phenotypes, potentially including the potential for tumorigenesis and/or differentiation.

FIG. 3. Heat map of miRNA expression in hES cells and their corresponding differentiated cells. Quantitative PCR of statistically significant miRNA candidates was performed on three independent hES cells lines and their corresponding differentiated cells. Expression of miRNA relative to the reference 2102Ep human EC cell line was determined and the $\log_2$ fold change depicted as a heat map with red representing higher and green lower levels of miRNA relative to the reference 2102Ep cell line (see color key, *inset*). Results were scaled by row (sample) and represented as the Z-score. Results confirm the ability to distinguish ES cells from their differentiated EB samples using this limited set of miRNAs.

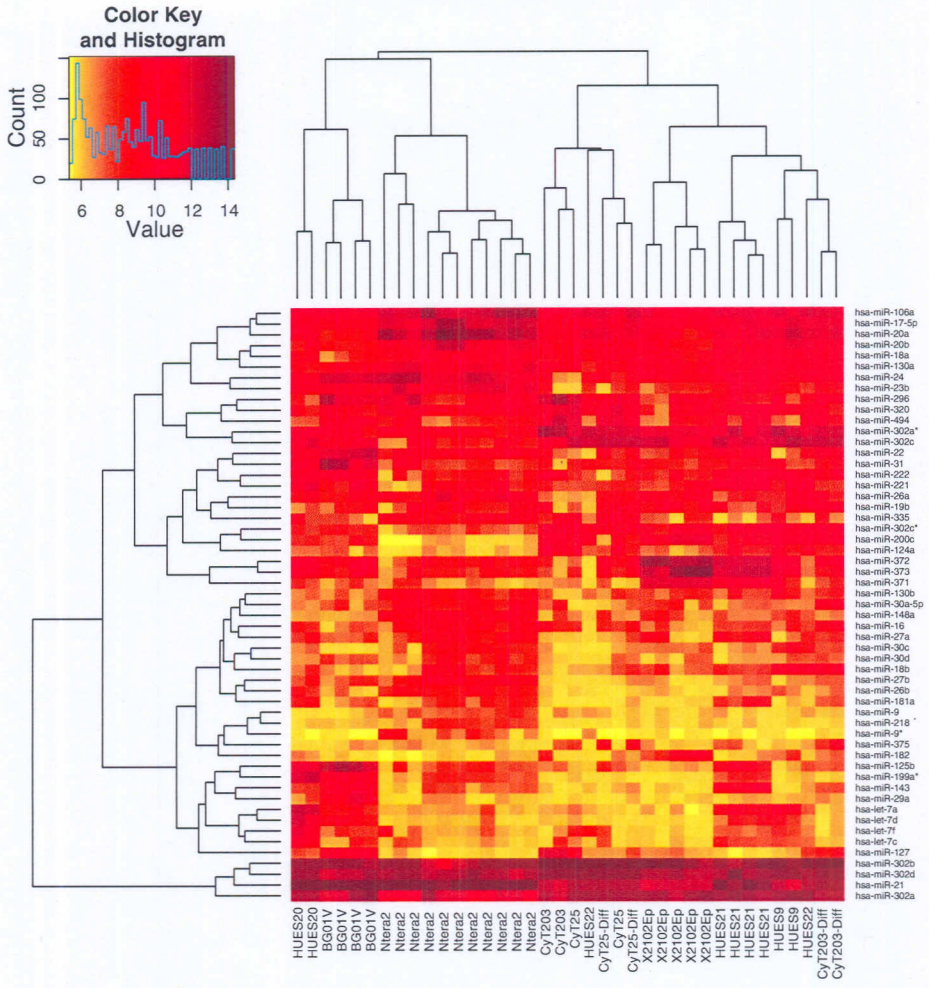
Color Key
and Histogram
Count
0
50
100
6
8
10
12
14
Value
hsa-miR-106a
hsa-miR-17-5p
hsa-miR-20a
hsa-miR-20b
hsa-miR-18a
hsa-miR-130a
hsa-miR-24
hsa-miR-23b
hsa-miR-296
hsa-miR-320
hsa-miR-494
hsa-miR-302a*
hsa-miR-302c
hsa-miR-22
hsa-miR-31
hsa-miR-222
hsa-miR-221
hsa-miR-26a
hsa-miR-19b
hsa-miR-335
hsa-miR-302c*
hsa-miR-200c
hsa-miR-124a
hsa-miR-372
hsa-miR-373
hsa-miR-371
hsa-miR-130b
hsa-miR-30a-5p
hsa-miR-148a
hsa-miR-16
hsa-miR-27a
hsa-miR-30c
hsa-miR-30d
hsa-miR-18b
hsa-miR-27b
hsa-miR-26b
hsa-miR-181a
hsa-miR-9
hsa-miR-218
hsa-miR-9*
hsa-miR-375
hsa-miR-182
hsa-miR-125b
hsa-miR-199a*
hsa-miR-143
hsa-miR-29a
hsa-let-7a
hsa-let-7d
hsa-let-7f
hsa-let-7c
hsa-miR-127
hsa-miR-302b
hsa-miR-302d
hsa-miR-21
hsa-miR-302a
HUES20
HUES20
BG01V
BG01V
BG01V
BG01V
Ntera2
Ntera2
Ntera2
Ntera2
Ntera2
Ntera2
Ntera2
Ntera2
Ntera2
CyT203
CyT203
CyT25
HUES22
CyT25-Diff
CyT25
CyT25-Diff
X2102Ep
X2102Ep
X2102Ep
X2102Ep
X2102Ep
HUES21
HUES21
HUES21
HUES21
HUES9
HUES9
HUES22
CyT203-Diff
CyT203-Diff

FIG. 2.

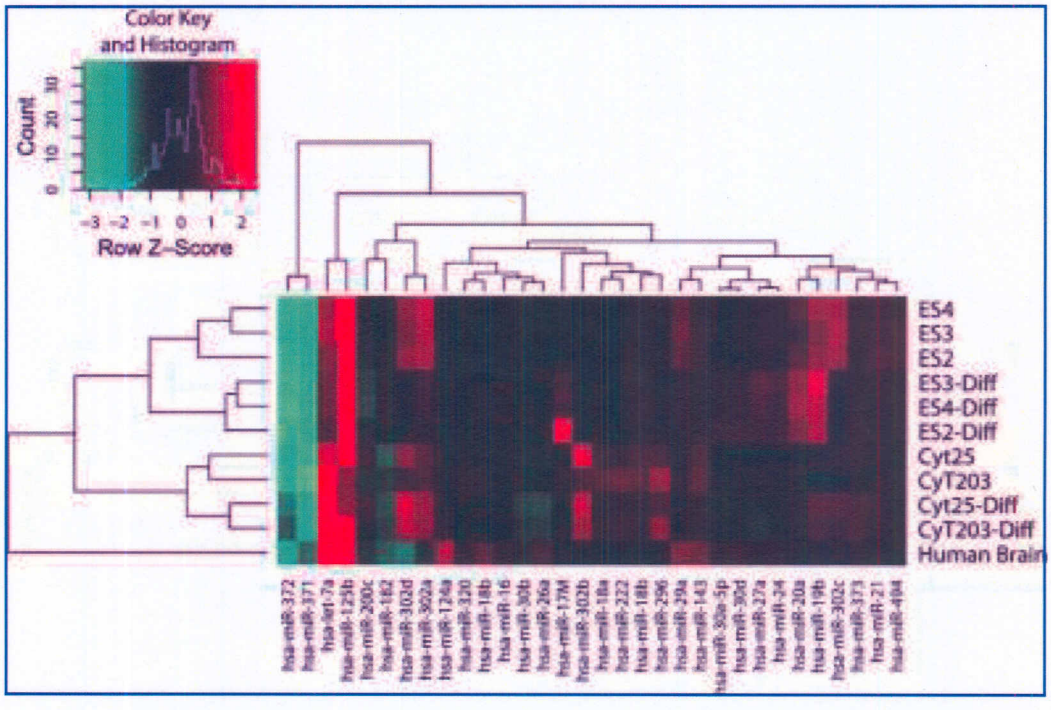
Color Key
and Histogram
Count
0
10
20
30
-3
-2
-1
0
1
2
Row Z-Score
ES4
ES3
ES2
ES3-Diff
ES4-Diff
ES2-Diff
Cyt25
CyT203
Cyt25-Diff
CyT203-Diff
Human Brain
hsa-miR-372
hsa-miR-371
hsa-let-7a
hsa-miR-125b
hsa-miR-200c
hsa-miR-182
hsa-miR-302d
hsa-miR-302a
hsa-miR-124a
hsa-miR-320
hsa-miR-18b
hsa-miR-16
hsa-miR-30b
hsa-miR-26a
hsa-miR-17M
hsa-miR-302b
hsa-miR-18a
hsa-miR-222
hsa-miR-18b
hsa-miR-296
hsa-miR-29a
hsa-miR-143
hsa-miR-30a-5p
hsa-miR-30d
hsa-miR-27a
hsa-miR-24
hsa-miR-20a
hsa-miR-19b
hsa-miR-302c
hsa-miR-373
hsa-miR-21
hsa-miR-494

FIG. 3.

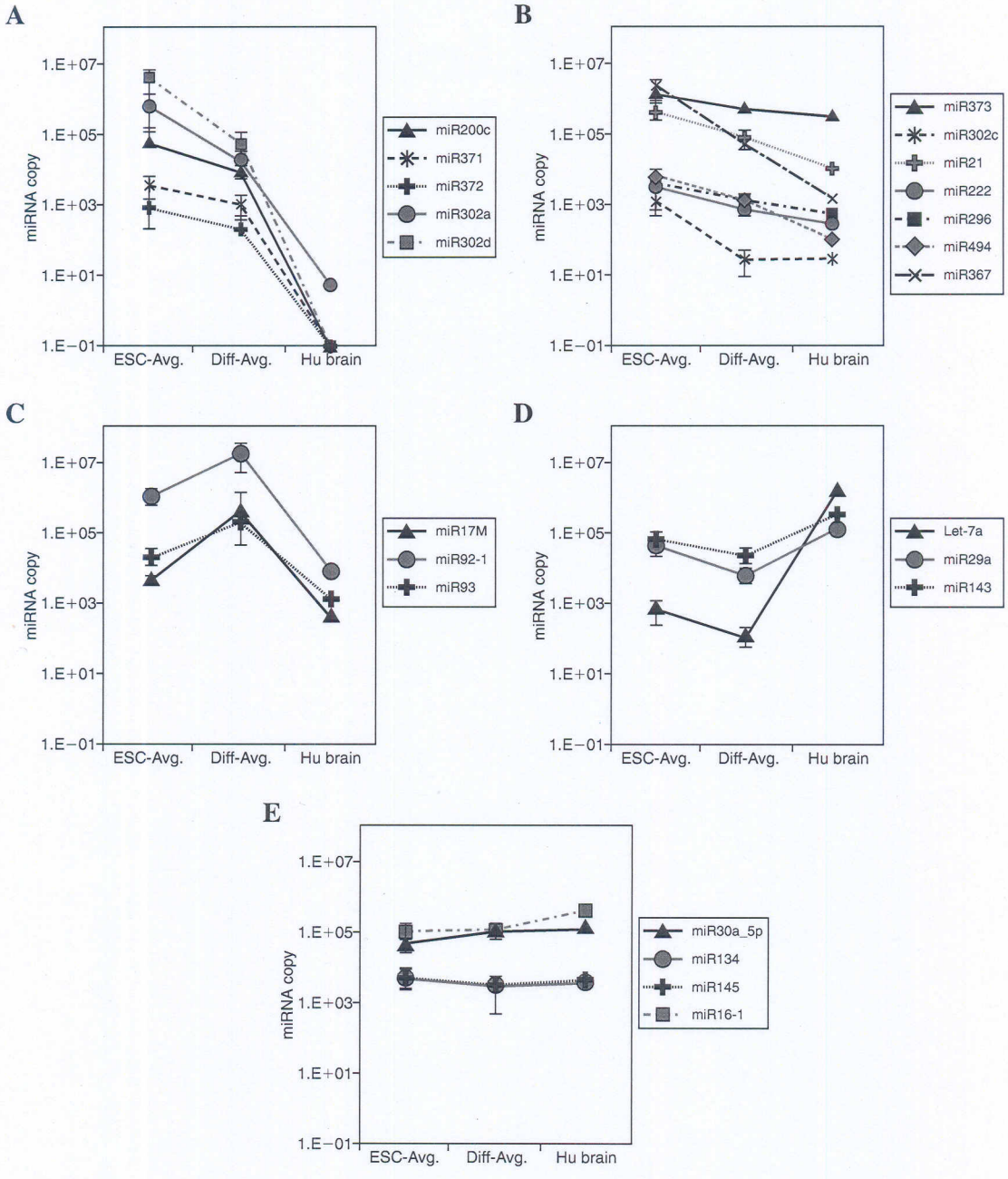

FIG. 4. Classification of differentially expressed markers between hES cells, differentiated cells and adult tissue (human brain). Relative expression of miRNAs compared to the standard 2102Ep control cells was calculated as fold change as described in Materials and Methods. A standard curve of a pure βAct fragment generated over 7 logs was used to deduce the copy number of miRNA in 2102Ep cells based on C_t values. These values were then used to determine the relative copy numbers in other samples using fold change values. (**A**) miRNAs highly expressed in hES cells decline with differentiation and are absent or present in very low levels in adult tissue. (**B**) miRNAs highly expressed in hES cells decline with differentiation and are present in relatively low levels in adult tissue. (**C**) miRNAs expressed in both hES cells and adult tissue with increasing levels in differentiated cells. Only miR-17 was significantly regulated, but two other members of the miR-17 cluster (33) were assayed for comparison. (**D**) miRNAs with relatively low expression in hES cells and differentiated cells compared to terminally differentiated adult tissue. (**E**) miRNAs expressed at comparable levels in hES cells, differentiated cells, and adult tissue.

ferences between multiple samples. Therefore, the fold change values for hES cells and differentiated samples were converted to copy numbers to reflect the abundance of candidate miRNAs in each sample. miRNA copy numbers were generated using a standard curve of a known miRNA and compared the miRNA quantitative PCR values from the 2102Ep sample against this standard. The fold-change (from 2102Ep) values of all cell-specific miRNA were then converted to approximate copy numbers by multiplication against the copy number value of each miRNA measured in the 2102Ep sample. Adult human brain tissue was included in the analysis as a representative of a terminally differentiated cell type.

Findings from this calculation show that the pattern of several miRNA was consistent across the undifferentiated ESC and differentiated cell sample pairs. The average copy number of selected miRNAs in the hES cell lines, their corresponding differentiated cells, and adult tissue is shown as a plot in Fig. 4 with the error bars representing the standard deviation between the samples. On the basis of miRNA expression differences between hES cells, differentiated cells, and adult tissue, candidate miRNAs can be divided into four main groups (Table 2). The first group of miRNA is highly expressed in hES cells with expression levels decreasing after differentiation and being undetectable in adult brain tissue (Fig. 4A). miRNAs in this group (302a, 302d, 371, 372, and 200c) have been reported to be associated with ES cells and EC cells in previous studies (15,16). A class of miRNAs under the first group is present at very high levels in hES cells with lower levels of expression in differentiated cells and adult tissue (Fig. 4B). In this group, a significant decrease in miR21, 222, 296, and 494 was noted changing from hES cells to differentiated cells. These miRNAs, while present, are significantly lower in adult tissue compared to hES cells and differentiated samples. In the second group, miRNAs are consistently expressed at higher levels in differentiated cells when compared with ES cells or adult tissue (Fig. 4C). Three miRNAs from a genomic cluster (33), 17M, 92 and 93, fall under this category, which may be indicative that these miRNAs play a role during the differentiation process. The third group of miRNAs is expressed at relatively low levels in hES cells and differentiated cells, but has increased expression in the adult brain tissue control. (Fig. 4D). Interestingly, Let7a, which is thought to be rare in pluripotent cells, was detected at varying levels in all the hES cells and differentiated cells. However, the level of Let-7 expression in hES cells was 3 logs lower than the adult tissue control. A fourth group consisting of miRNAs, such as miR16, 134, 246, and 30a_5p, was found to be expressed at relatively comparable levels in hES cells, differentiated cells, and adult brain tissue (Fig.4E), suggesting that they may be involved in general cellular function.

Cross-correlation of mRNA and miRNA

To determine potential correlation of mRNA expression and miRNA expression, the data generated from this study were combined with data reported in an earlier study, including several hES cells lines and hEC lines (48), and modeled for cross-correlation. We reasoned that miRNAs and mRNAs that are coordinately regulated or mRNAs that are targeted for destruction by specific miRNAs ought to exhibit distinct patterns of correlated levels over specific cell types or conditions. Therefore, we modeled the data to examine these correlations most appropriately.

A linear model was fit to the log-expression profile of each mRNA or miRNA, where additive effects for each experiment group were estimated via least squares. Undifferentiated hES cells lines (HUES9, HUES20, HUES22, BG0V1, CyT25, and CyT203) comprised the baseline group, whereas differentiated CyT25 and differentiated CyT203 comprised two separate groups. Finally, Ntera2 and 2102Ep formed the last two groups, for a total of five groups. An F-test was used to select differentially expressed genes (that differ between at least two of the biological groups). The p values were adjusted for multiple comparisons using the Benjamini–Hochberg method at 5% FDR, resulting in 55 miRNAs and 2,678 mRNAs. The miRNA/mRNA data were jointly examined by computing pairwise correlations between the esti-

TABLE 2. miRNAs SPECIFIC TO hES CELLS OR DIFFFERENTIATED CELLS BASED ON NCODE™ QUANTITATIVE PCR PROFILES

miRNA	*ESC*	*Diff*	*Adult tissue*	*Known function*
miR200c, 371, 372, 302a, 320d	High	Low	Absent	Present in hES cells and EC (16)
miR373, 302c, 21, 222, 296, 494, 367	High	Low	Lower	Inhibits erythroblast formation; Antiapoptotic factor (72, 73)
miR154, 29a, 143, 29c, Let7a	High	Low	High	Present in MEF/NIH3T3,; Promotes adipocyte diff (15, 36)
miR17M, 92, 93	Low	Higher	Low	Reported in single mESC (17)
miR16, 134, 145, 30a_5p	Same	Same	Same	General Cellular Function (?)

mated additive effect profiles (results shown in Supplementary Table 4, accessible at http://cord.rutgers.edu/appendix/Supplemental_Table_4.xls). A heat map depicting the cross-correlation of the entire set of significant genes is shown in Supplementary Fig. 1 (accessible at http://cord.rutgers.edu/appendix/Supplemental_Figure1.pdf). Although the number of genes depicted makes it impossible to label specific mRNAs, it is clear that identifiable clusters of mRNAs and miRNA emerge from the analysis as regions of positive correlations (red) and negative correlations (green). Perhaps these relationships will be simpler to examine if we focus on an understandable subset of the significant mRNAs.

Using a list of pluripotency, germ line-specific, and general differentiation markers (54), we selected 40 genes from the significant mRNA list and redrew the heat map using correlations to all 55 miRNAs (Fig. 5). Again, clear patterns of positive and negative correlations were identified (red and green regions, respectively). Using this cross-clustering technique, mRNAs are clustered according to their cell-specific expression pattern (54) nearly perfectly (see the color coding to the left of the heat map in Fig. 5). Similarly, miRNAs are divided into two major clusters. Within these groups, polycistronic family members are clustered together, miRNAs derived from the same hairpin precursor cluster together, and the ES-specific miR-302 family is both positively correlated with ES-specific mRNA markers and negatively correlated with EB mRNA markers.

If expression correlations imply the possibility of a functional interaction, we might predict that miRNAs within clusters of negative correlation (red) should have a preponderance of predicted mRNA targets. Using the target predictions from the RNA22 algorithm (53), we do not see a clear prevalence of targets corresponding to regions of negative correlations. Some target predictions support roles for previously described stem-specific miRNAs. For example, the ES-specific miR-302 family (15,16) is relatively devoid of predicted targets, consistent with a role in suppressing mRNAs that are not present or not regulated in these conditions. The miR-302 family, among several other significantly regulated miRNAs, is predicted to target the mRNA encoding laminin (LAMC1). Laminin expression and binding to integrin is important for cell–cell interactions during EB formation (58,59), so expression of laminin ought to be repressed in a stem cell and should be tightly regulated. However, other than select cases such as laminin, there is no overall association of negative correlation with target prediction. Our results, therefore, are consistent with the conclusion that negative correlations of miRNA and mRNA do not directly predict functional targeting, but may identify valuable targeting predictions worth investigating further.

DISCUSSION

Here we have used a combination of NCode™ miRNA array and quantitative PCR to identify and validate miRNAs differentially expressed between multiple cell states. The identified miRNA markers were quantitatively measured in five independent hES cells lines using quantitative RT-PCR.

On the basis of the expression pattern in ES cells, differentiated cells, and adult brain, three main groups of differentially expressed miRNAs were identified. Group one miRNA (Fig. 4A,B, similar to cluster 4 in Fig. 5) are expressed at relatively high copy number in hES cells and then seem to be down-regulated during differentiation. These miRNAs represent good candidates for markers of pluripotency and potentially negative regulators of gene expression that may play a role in restricting differentiation of hES cells. Indeed, they positively cross-correlate with Oct-4 (POU5F1), Rex1 (ZFP42), and TDGF1, which may also be considered to be markers of pluripotency. Group two miRNAs (Fig. 4C, also cluster 3 in Fig. 5) are expressed at intermediate levels in hES cells and significantly increase in copy number during differentiation. The expression level of these miRNAs is relatively low in the representative adult control tissue when compared to differentiating cells. This group positively correlates with two Hox family members, CDX2 and HOXA11, which may be transiently expressed during early differentiation and reduced afterward. Finding similarities between the copy number and the intermediate differentiation state allows one to speculate that these molecules could represent a class of miRNAs that act to regulate differentiation of cells to one or more of the three embryonic lineages. Group three miRNAs (Fig. 4C) decreased after differentiation but do not seem to be specifically associated with the ES cell state because they are also expressed at significant levels in adult tissue.

Regulation of gene expression by miRNA is clearly a complex process, as indicated by the ability of an individual miRNA candidate to regulate several mRNA targets (60) or several miRNAs able to regulate a single mRNA (61). The mechanism of miRNA-mediated mRNA regulation itself might be either by inhibition of transcription due to chromatin modification, DNA methylation or direct translational inhibition of the mRNA (62–65). The latter can be due to repression or cleavage of target mRNA whereby the extent of base pairing between the miRNA and the mRNA determines the balance between cleavage and degradation of the transcript (66,67). Considering this complexity, it is difficult to identify functionally relevant gene targets for candidate miRNAs. Despite the identification of several miRNAs in specific cell types and sequence-based prediction of possible regulatory targets (61,68–70), verification of specific activity

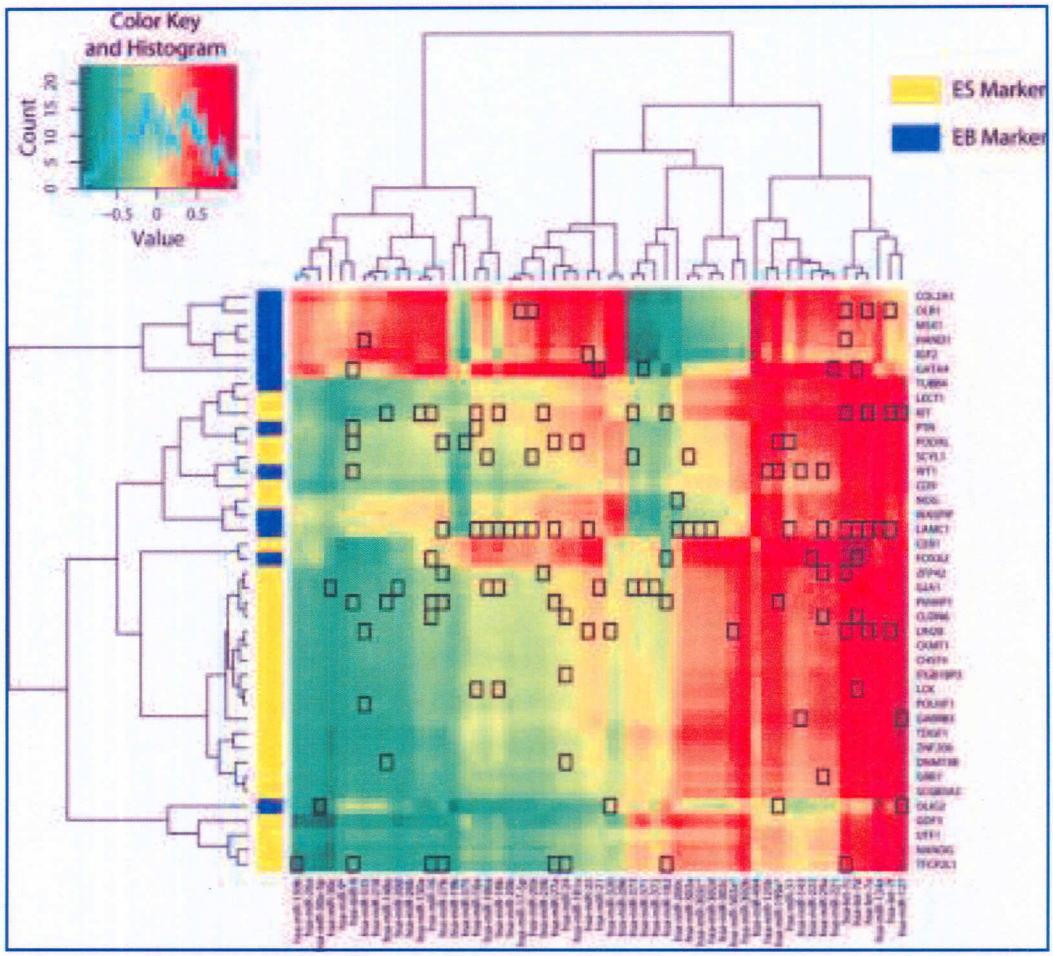

FIG. 5. Cross-correlation heat map of selected mRNA and miRNA expression patterns. A cross-correlation table (Supplementary Table 4, accessible at http://cord.rutgers.edu/appendix/Supplemental_Table_4.xds) was constructed for all 2,678 selected mRNAs and 55 miRNAs and expressed as a heatmap (Supplementary Fig. 1, accessible at http://cord.rutgers.edu/appendix/Supp_Figure_1.pdf). Here, a subset of mRNAs specific for pluripotency, germ-line-specific, and general differentiation markers was selected and used to construct a heat map, colored by the Pearson correlation coefficient (*R*-value; see color key, *inset*). Specific mRNAs were color coded (left) as being ES-specific (yellow) or EB-specific (blue) on the basis of previous studies (54). Target predictions computed using the RNA22 algorithm (53) are identified by drawing a box around the correlation cell at the intersection of the miRNA and the predicted mRNA target.

has been difficult because there are many potential targets for each candidate miRNA. For example, miR-200c, which is expressed at high levels in hES cells, has 567 gene targets predicted by RNA22 (53). Of those present among the Illumina probe set, 33% were reliably detected in all hES cell samples, suggesting the presence of both the miRNA and the predicted targets, thus providing the possibility of interaction. However, this analysis focused on only one miRNA and one condition. If we expand our view, we can group miRNAs through their association with many mRNAs under multiple conditions more specifically, analogous to the concept of "biclustering" (71). In our method, correlation of an mRNA to each miRNA expression level is used as a "condition" to help reveal associations between mRNAs. The inverse is applied to miRNAs as well. Therefore, cross-correlation clustering presents interpretable lists of miRNAs and associated mRNAs that may be hypothesized to interact through specific mechanisms. Such is the case in Fig. 5, where mRNAs indicative of pluripotency are negatively associated with miRNAs predicted to target these mRNAs, and positively associated with miRNAs predicted to regulate other genes coordinately. This view of the data, while somewhat superficial, provides the initial impetus toward a systems analysis to recognize the role of miRNAs in stem cell differentiation.

In conclusion, miRNA analysis represents a relatively new tool for cell line profiling and discovery of putative regulatory molecules. In addition, it provides a method to study and dissect the epigenetic regulation mechanisms involved in maintenance and differentiation of hES cells. Such an insight is essential in developing methods either to maintain cells in their pluripotent undifferentiated state or to differentiate them efficiently into a desired lineage.

ACKNOWLEDGMENTS

We thank Dr. Melissa Carpenter, Novocell, for providing us with the undifferentiated and differentiated cell pellets of CyT25 and CyT203 cells; Dr. Chris Adams and Mark Landers, Invitrogen, for their technical help with NCode™ miRNA profiling tools; and Drs. Bruce Davidson and Jeremy Crook, ES Cell International, for their excellent editorial advice. R.P.H. was supported by grants from the New Jersey Commission on Spinal Cord Research, National Institutes of Health, the New Jersey Commission on Science & Technology, and Invitrogen, Inc.

REFERENCES

1. Rao S and SH Orkin. (2006). Unraveling the transcriptional network controlling ES cell pluripotency. Genome Biol 7:230.
2. Xiao L, X Yuan and SJ Sharkis. (2006). Activin A maintains self-renewal and regulates fibroblast growth factor, Wnt, and bone morphogenic protein pathways in human embryonic stem cells. Stem Cells 24:1476–1486.
3. Bibikova M, E Chudin, B Wu, L Zhou, EW Garcia, Y Liu, S Shin, TW Plaia, JM Auerbach, DE Arking, R Gonzalez, J Crook, B Davidson, TC Schulz, A Robins, A Khanna, P Sartipy, J Hyllner, P Vanguri, S Savant-Bhonsale, AK Smith, A Chakravarti, A Maitra, M Rao, DL Barker, JF Loring and JB Fan. (2006). Human embryonic stem cells have a unique epigenetic signature. Genome Res 16:1075–1083.
4. Lagarkova MA, PY Volchkov, AV Lyakisheva, ES Philonenko and SL Kiselev. (2006). Diverse epigenetic profile of novel human embryonic stem cell lines. Cell Cycle 5:416–420.
5. Ciaudo C, A Bourdet, M Cohen-Tannoudji, HC Dietz, C Rougeulle and P Avner. (2006). Nuclear mRNA degradation pathway(s) are implicated in Xist regulation and X chromosome inactivation. PLoS Genet 2:e94.
6. Enver T, S Soneji, C Joshi, J Brown, F Iborra, T Orntoft, T Thykjaer, E Maltby, K Smith, RA Dawud, M Jones, M Matin, P Gokhale, J Draper and PW Andrews. (2005). Cellular differentiation hierarchies in normal and culture-adapted human embryonic stem cells. Hum Mol Genet 14:3129–3140.
7. Brimble SN, X Zeng, DA Weiler, Y Luo, Y Liu, IG Lyons, WJ Freed, AJ Robins, MS Rao and TC Schulz. (2004). Karyotypic stability, genotyping, differentiation, feeder-free maintenance, and gene expression sampling in three human embryonic stem cell lines derived prior to August 9, 2001. Stem Cells Dev 13:585–597.
8. Ludwig TE, V Bergendahl, ME Levenstein, J Yu, MD Probasco and JA Thomson. (2006). Feeder-independent culture of human embryonic stem cells. Nature Methods 3:637–646.
9. Abeyta MJ, AT Clark, RT Rodriguez, MS Bodnar, RA Pera and MT Firpo. (2004). Unique gene expression signatures of independently-derived human embryonic stem cell lines. Hum Mol Genet 13:601–608.
10. Bhattacharya B, J Cai, Y Luo, T Miura, J Mejido, SN Brimble, X Zeng, TC Schulz, MS Rao and RK Puri. (2005). Comparison of the gene expression profile of undifferentiated human embryonic stem cell lines and differentiating embryoid bodies. BMC Dev Biol 5:22.
11. Liu Y, S Shin, X Zeng, M Zhan, R Gonzalez, FJ Mueller, CM Schwartz, H Xue, H Li, SC Baker, E Chudin, DL Barker, TK McDaniel, S Oeser, JF Loring, MP Mattson and MS Rao. (2006). Genome wide profiling of human embryonic stem cells (hES cells), their derivatives and embryonal carcinoma cells to develop base profiles of U.S. Federal government approved hES cells lines. BMC Dev Biol 6:20.
12. Richards M, SP Tan, JH Tan, WK Chan and A Bongso. (2004). The transcriptome profile of human embryonic stem cells as defined by SAGE. Stem Cells 22:51–64.
13. Skottman H, M Mikkola, K Lundin, C Olsson, AM Stromberg, T Tuuri, T Otonkoski, O Hovatta and R Lahesmaa. (2005). Gene expression signatures of seven individual human embryonic stem cell lines. Stem Cells 23:1343–1356.
14. Wei CL, T Miura, P Robson, SK Lim, XQ Xu, MY Lee, S Gupta, L Stanton, Y Luo, J Schmitt, S Thies, W Wang, I Khrebtukova, D Zhou, ET Liu, YJ Ruan, M Rao and B Lim. (2005). Transcriptome profiling of human and murine ESCs identifies divergent paths required to maintain the stem cell state. Stem Cells 23:166–185.
15. Houbaviy HB, MF Murray and PA Sharp. (2003). Embryonic stem cell-specific MiRNAs. Dev Cell 5:351–358.
16. Suh MR, Y Lee, JY Kim, SK Kim, SH Moon, JY Lee, KY Cha, HM Chung, HS Yoon, SY Moon, VN Kim and KS Kim. (2004). Human embryonic stem cells express a unique set of miRNAs. Dev Biol 270:488–498.
17. Tang F, P Hajkova, SC Barton, K Lao and MA Surani. (2006). MiRNA expression profiling of single whole embryonic stem cells. Nucleic Acids Res 34:e9.
18. Kim VN and JW Nam. (2006). Genomics of miRNA. Trends Genet 22:165–173.
19. Aukerman MJ and H Sakai. (2003). Regulation of flowering time and floral organ identity by a MiRNA and its APETALA2-like target genes. Plant Cell 15:2730–2741.
20. Bagga S, J Bracht, S Hunter, K Massirer, J Holtz, R Eachus and AE Pasquinelli. (2005). Regulation by let-7 and lin-4 miRNAs results in target mRNA degradation. Cell 122:553–563.
21. Chen CZ, L Li, HF Lodish and DP Bartel. (2004). MiRNAs modulate hematopoietic lineage differentiation. Science 303:83–86.
22. Yekta S, IH Shih and DP Bartel. (2004). MiRNA-directed cleavage of HOXB8 mRNA. Science 304:594–596.

23. Yu Z, T Raabe and NB Hecht. (2005). MiRNA Mirn122a reduces expression of the posttranscriptionally regulated germ cell transition protein 2 (Tnp2) messenger RNA (mRNA) by mRNA cleavage. Biol Reprod 73:427–433.
24. Giraldez AJ, Y Mishima, J Rihel, RJ Grocock, S Van Dongen, K Inoue, AJ Enright and AF Schier. (2006). Zebrafish MiR-430 promotes deadenylation and clearance of maternal mRNAs. Science 312:75–79.
25. Wu L, J Fan and JG Belasco. (2006). MiRNAs direct rapid deadenylation of mRNA. Proc Natl Acad Sci USA 103:4034–4039.
26. Zhang B, X Pan and TA Anderson. (2006). MiRNA: A new player in stem cells. J Cell Physiol 209:266–269.
27. Bartel DP. (2004). MiRNAs: Genomics, biogenesis, mechanism, and function. Cell 116:281.
28. Wu L and JG Belasco. (2005). Micro-RNA regulation of the mammalian lin-28 gene during neuronal differentiation of embryonal carcinoma cells. Mol Cell Biol 25:9198–9208.
29. Cheng AM, MW Byrom, J Shelton and LP Ford. (2005). Antisense inhibition of human miRNAs and indications for an involvement of miRNA in cell growth and apoptosis. Nucleic Acids Res 33:1290–1297.
30. Sullivan CS and D Ganem. (2005). MiRNAs and viral infection. Mol Cell 20:3–7.
31. Calin GA, CD Dumitru, M Shimizu, R Bichi, S Zupo, E Noch, H Aldler, S Rattan, M Keating, K Rai, L Rassenti, T Kipps, M Negrini, F Bullrich and CM Croce. (2002). Frequent deletions and down-regulation of micro-RNA genes miR15 and miR16 at 13q14 in chronic lymphocytic leukemia. Proc Natl Acad Sci USA 99:15524–15529.
32. Calin GA, C Sevignani, CD Dumitru, T Hyslop, E Noch, S Yendamuri, M Shimizu, S Rattan, F Bullrich, M Negrini and CM Croce. (2004). Human miRNA genes are frequently located at fragile sites and genomic regions involved in cancers. Proc Natl Acad Sci USA 101:2999–3004.
33. He L, JM Thomson, MT Hemann, E Hernando-Monge, D Mu, S Goodson, S Powers, C Cordon-Cardo, SW Lowe, GJ Hannon and SM Hammond. (2005). A miRNA polycistron as a potential human oncogene. Nature 435:828–833.
34. Berezikov E, V Guryev, J van de Belt, E Wienholds, RH Plasterk and E Cuppen. (2005). Phylogenetic shadowing and computational identification of human miRNA genes. Cell 120:21–24.
35. Hatfield SD, HR Shcherbata, KA Fischer, K Nakahara, RW Carthew and H Ruohola-Baker. (2005). Stem cell division is regulated by the miRNA pathway. Nature 435:974–978.
36. Esau C, X Kang, E Peralta, E Hanson, EG Marcusson, LV Ravichandran, Y Sun, S Koo, RJ Perera, R Jain, NM Dean, SM Freier, CF Bennett, B Lollo and R Griffey. (2004). MiRNA-143 regulates adipocyte differentiation. J Biol Chem 279:52361–52365.
37. Zhao Y, E Samal and D Srivastava. (2005). Serum response factor regulates a muscle-specific miRNA that targets Hand2 during cardiogenesis. Nature 436:214–220.
38. Kuwabara T, J Hsieh, K Nakashima, K Taira and FH Gage. (2004). A small modulatory dsRNA specifies the fate of adult neural stem cells. Cell 116:779–793.
39. Chen CZ and HF Lodish. (2005). MiRNAs as regulators of mammalian hematopoiesis. Semin Immunol 17:155–165.
40. Kanellopoulou C, SA Muljo, AL Kung, S Ganesan, R Drapkin, T Jenuwein, DM Livingston and K Rajewsky. (2005). Dicer-deficient mouse embryonic stem cells are defective in differentiation and centromeric silencing. Genes Dev 19:489–501.
41. Murchison EP, JF Partridge, OH Tam, S Cheloufi and GJ Hannon. (2005). Characterization of Dicer-deficient murine embryonic stem cells. Proc Natl Acad Sci USA 102:12135–12140.
42. Yang S, S Tutton, E Pierce and K Yoon. (2001). Specific double-stranded RNA interference in undifferentiated mouse embryonic stem cells. Mol Cell Biol 21:7807–7816.
43. Wang Y, R Medvid, C Melton, R Jaenisch and R Blelloch. (2007). DGCR8 is essential for miRNA biogenesis and silencing of embryonic stem cell self-renewal. Nature Genet 39:380–385.
44. Goff LA, M Yang, J Bowers, RC Getts, RW Padgett and RP Hart. (2005). Rational probe optimization and enhanced detection strategy for miRNAs using microarrays. RNA Biol 2:e9–.e16.
45. D'Amour KA, AG Bang, S Eliazer, OG Kelly, AD Agulnick, NG Smart, MA Moorman, E Kroon, MK Carpenter and EE Baetge. (2006). Production of pancreatic hormone-expressing endocrine cells from human embryonic stem cells. Nature Biotechnol 24:1392–1401.
46. Reubinoff BE, MF Pera, CY Fong, A Trounson and A Bongso. (2000). Embryonic stem cell lines from human blastocysts: somatic differentiation in vitro. Nature Biotechnol 18:399–404.
47. Costa M, M Dottori, E Ng, SM Hawes, K Sourris, P Jamshidi, MF Pera, AG Elefanty and EG Stanley. (2005). The hES cells line Envy expresses high levels of GFP in all differentiated progeny. Nature Methods 2:259–260.
48. Josephson R, CJ Ording, Y Liu, S Shin, U Lakshmipathy, A Toumadje, B Love, JD Chesnut, PW Andrews, MS Rao and JM Auerbach. (2007). Comprehensive characterization of a reference line for human embryonic stem cell research-2102Ep human embryonal carcinoma line. Stem Cells 25:437–446.
49. Lakshmipathy U, B Love, C Adams, B Thyagarajan and JD Chesnut. (2006). MiRNA profiling: an easy and rapid method to screen and characterize stem cell populations. In: *Stem Cell Assays*. V M.C., ed. Humana Press, New Jersey.
50. Bolstad BM, RA Irizarry, M Astrand and TP Speed. (2003). A comparison of normalization methods for high density oligonucleotide array data based on variance and bias. Bioinformatics (Oxford, England) 19:185–193.
51. Cui X, MK Kerr and GA Churchill. (2003). Transformations for cDNA microarray data. Statistical applications in genetics and molecular biology 2:Article4.
52. Benjamini Y and Y Hochberg. (1995). Controlling the False Discovery Rate - A Practical and Powerful Approach to Multiple Testing. J R Statist Soc Ser B-Methodological 57:289.
53. Miranda KC, T Huynh, Y Tay, YS Ang, WL Tam, AM Thomson, B Lim and I Rigoutsos. (2006). A pattern-based method for the identification of MiRNA binding sites and their corresponding heteroduplexes. Cell 126:1203–1217.

54. Cai J, J Chen, Y Liu, T Miura, Y Luo, JF Loring, WJ Freed, MS Rao and X Zeng. (2006). Assessing self-renewal and differentiation in human embryonic stem cell lines. Stem Cells 24:516–530.
55. Si ML, S Zhu, H Wu, Z Lu, F Wu and YY Mo. (2006). miR-21-mediated tumor growth. Oncogene 26:2799–2803.
56. Zhu S, ML Si, H Wu and YY Mo. (2007). MiRNA-21 targets the tumor suppressor gene tropomyosin 1 (TPM1). J Biol Chem 282:14328–14336.
57. Krichevsky AM, KS King, CP Donahue, K Khrapko and KS Kosik. (2003). A miRNA array reveals extensive regulation of miRNAs during brain development. RNA 9:1274.
58. Colognato H and PD Yurchenco. (2000). Form and function: the laminin family of heterotrimers. Dev Dyn 218:213–234.
59. Li S, D Harrison, S Carbonetto, R Fassler, N Smyth, D Edgar and PD Yurchenco. (2002). Matrix assembly, regulation, and survival functions of laminin and its receptors in embryonic stem cell differentiation. J Cell Biol 157:1279–1290.
60. Lim LP, NC Lau, P Garrett-Engele, A Grimson, JM Schelter, J Castle, DP Bartel, PS Linsley and JM Johnson. (2005). Microarray analysis shows that some miRNAs downregulate large numbers of target mRNAs. Nature 433:769–773.
61. Lewis BP, IH Shih, MW Jones-Rhoades, DP Bartel and CB Burge. (2003). Prediction of mammalian miRNA targets. Cell 115:787–798.
62. Hall KB. (2002). RNA-protein interactions. Curr Opin Struct Biol 12:283–288.
63. Jones S, DT Daley, NM Luscombe, HM Berman and JM Thornton. (2001). Protein-RNA interactions: a structural analysis. Nucleic Acids Res 29:943–954.
64. Mette MF, W Aufsatz, J van der Winden, MA Matzke and AJ Matzke. (2000). Transcriptional silencing and promoter methylation triggered by double-stranded RNA. EMBO J 19:5194–5201.
65. Volpe TA, C Kidner, IM Hall, G Teng, SI Grewal and RA Martienssen. (2002). Regulation of heterochromatic silencing and histone H3 lysine-9 methylation by RNAi. Science 297:1833–1837.
66. Doench JG and PA Sharp. (2004). Specificity of miRNA target selection in translational repression. Genes Dev 18:504–511.
67. Hutvagner G and PD Zamore. (2002). A miRNA in a multiple-turnover RNAi enzyme complex. Science 297:2056–2060.
68. John B, AJ Enright, A Aravin, T Tuschl, C Sander and DS Marks. (2004). Human MiRNA targets. PLoS Biol 2:e363.
69. Kiriakidou M, PT Nelson, A Kouranov, P Fitziev, C Bouyioukos, Z Mourelatos and A Hatzigeorgiou. (2004). A combined computational-experimental approach predicts human miRNA targets. Genes Dev 18:1165–1178.
70. Smalheiser NR and VI Torvik. (2004). A population-based statistical approach identifies parameters characteristic of human miRNA-mRNA interactions. BMC Bioinformatics 5:139.
71. Cheng Y and GM Church. (2000). Biclustering of expression data. Proceedings / International Conference on Intelligent Systems for Molecular Biology; ISMB 8:93–103.
72. Chan JA, AM Krichevsky and KS Kosik. (2005). MiRNA-21 is an antiapoptotic factor in human glioblastoma cells. Cancer Res 65:6029–6033.
73. Felli N, L Fontana, E Pelosi, R Botta, D Bonci, F Facchiano, F Liuzzi, V Lulli, O Morsilli, S Santoro, M Valtieri, GA Calin, CG Liu, A Sorrentino, CM Croce and C Peschle. (2005). MiRNAs 221 and 222 inhibit normal erythropoiesis and erythroleukemic cell growth via kit receptor down-modulation. Proc Natl Acad Sci USA 102:18081–18086.

Address reprint requests to:
Dr. Uma Lakshmipathy
Invitrogen Corporation
1600 Faraday Avenue
Carlsbad, CA 92008

E-mail: uma.lakshmipathy@invitrogen.com

Received for publication February 6, 2007; accepted after revision May 8, 2007.